

# Femtocell Interference and Probability of Connection in different Areas and Various SINR Threshold Values at Downlink

<sup>1</sup>Mohammed Alshami, <sup>2</sup>Tughrul Arslan, and <sup>3</sup>John Thompson

<sup>1</sup> School of Engineering, The University of Edinburgh, Edinburgh, UK

<sup>2</sup> School of Engineering, The University of Edinburgh, Edinburgh, UK

<sup>3</sup> School of Engineering, The University of Edinburgh, Edinburgh, UK

E-mail address: m.h.alshami@ed.ac.uk, t.arslan@ed.ac.uk, john.thompson@ed.ac.uk

Received 23 Sept 2013, Revised 20 Oct 2013, Accepted 13 Nov 2013, Published 1 Jan 2014

**Abstract:** The increasing requirements for higher data rates in cellular systems lead wireless communication companies to invent femtocell (FMC) which is a small cell size. FMC is a low power cellular home base station, low in cost, operating within a licensed spectrum and designed for use in residential or small business areas, both indoors and outdoors, and deployed to improve cellular system coverage. FMC has been deployed extensively and is included in the Long Term Evolution (LTE) and the Worldwide Interoperability Microwave Access (WiMAX) networks for indoors. This paper presents the interference, SINR and the probability of connection at the downlink for a varying number of FMCs based on the LTE and WiMAX OFDMA range. Moreover, the comparison of interference, SINR and probability of connection are studied for three different indoor areas. In addition, a comparison for the probability of connection with various threshold values and various number of FMCs is simulated and presented in 3-D. The downlink interference occurs from neighbouring FMCs to the target user equipment (UE), when the signal transmits from the serving FMC to the target UE and the signals which are transmitted from the neighbouring FMCs would have the same subchannels during the downlink transmission.

**Keywords:** Femtocell, Home Base Station, Interference, SINR, UserEquipment, Indoors, OFDMA, Downlink

## I. INTRODUCTION

The concept of FMC was known as a home base station access point with low power installed at home by users to give more coverage and increase the data rate capacity. FMC was deployed and included in LTE and WiMAX networks in the indoors. FMC capacity indoors is more than that from LTE or WiMAX macro base station (BS), because to receive indoors from BS we need more power that will lead to reduced capacity. FMC will save UE power as the distance is very short compared to the distance to BS and it is important as it can provide coverage to area that BS cannot reach. Public could access FMC and UE outdoors could connect with the FMC network indoors easier than connect with BS. FMC coverage distance is between 10 m and 30 m. FMC installed at home or in an office by subscribers without need for operators and it serves up to 4 users. FMC is deployed mainly indoors and sometimes outdoors at the LTE or WiMAX base station (BS) cell edge to increase

the area of coverage, data rate capacity and in order to enhance the received signal in the user's premises,[1-3].

No similar work has been carried out. One of the issues that affect the performance of FMC is the interference. In previous contributions, FMC deployment is inspected without detail with respect to interference; signal to interference and noise ratio (SINR) and without finding the probability of connection. However, [4] evaluated the interference for frames and calculated the throughput and [5] discussed the path loss of FMCs indoors. The work in this paper evaluates the interference for subcarriers and calculates the SINR and the probability of connection for a varied number of FMCs and a specific indoors area between the femtocells and the user equipment devices. Moreover, this work compares the interference SINR and the probability of connection at various indoors areas and compares the probability of connection in 3-dimensions at various SINR threshold values and various numbers of FMCs [6-10].

The remainder of this paper is organized as follows. Section 2 introduces the downlink FMC system model. Section 3 explains the downlink FMC interference. Section 4 provides the downlink simulation scenario. Section 5 summaries and concludes the journal.

## II. DOWNLINK FEMTOCELL SYSTEM MODEL

### A. Interference Concept

When FMCs and UEs transmit their signals in the same frequency band within the same environment, interference will occur in the deployment of FMCs due to use of the same carrier frequency. Nevertheless, constraint will occur throughout the transmission of signals due to interference which will happen in the deployment when a number of FMCs transmit their signals in the same frequency band within the same area [11, 12]. Even though interference is the main challenge that faces the deployment of FMCs, the advantages of FMCs deployment is the increase in coverage and the improvement of capacity, while the disadvantages are the high probability of interference in the absence of network design [13-15].

### B. Terminology

The terms used in this paper are listed as in Table I.

TABLE I. SUMMARY OF TERMINOLOGY USED IN THIS PAPER

Terms	Description
BS	LTE or WiMAX macro base station
FMC	Femtocell home base station access point
UE	Femtocell user equipment device
BS <sub>UE</sub>	LTE or WiMAX macro base station user equipment device
FMC-UE	Interference transmitted from interferer Femtocells to target user equipment
UEs-FMC	Interference transmitted from interferers user equipment devices to serving Femtocell
FMC-BS	Interference transmitted from FMC to LTE or WiMAX macro base station
BS-FMC <sub>UE</sub>	Interference transmitted from LTE or WiMAX macro base station to FMCuser equipment device

### C. FMC Coverage

FMC provides extension of the coverage within strength for the signal. FMCs were designed and implemented as a solution to extend and provide better quality indoor network coverage [16, 17].

### D. Downlink OFDMA

FMCs transmits in different subcarriers than BS in OFDMA systems, which help in interference avoidance. In addition, in OFDMA system, FMCs are deployed in subchannels distribution. In downlink the UE which is indoors and receiving signal from indoor FMC must have different subchannels from the UE which is outdoors and receiving signal directly from the outdoors BS [18].

## III. DOWNLINK FEMTOCELL INTERFERENCE

### A. Co-Layer Interference

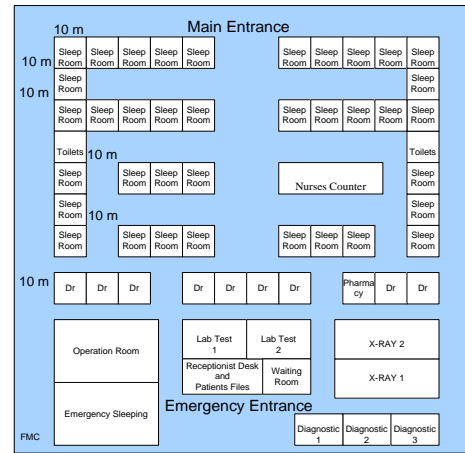
Co-Layer interference is the transmission of signals from different FMCs at the same layer [19]. Co-Layer interference occurs in downlink when the signal is transmitted from the serving FMC to the target UE and is not strong enough compared to the interference coming from the neighbors FMCs to the target UE, when the serving FMC and the neighbor FMC are transmitted at the same subchannel .

### B. BS - FMC<sub>UE</sub> Interference

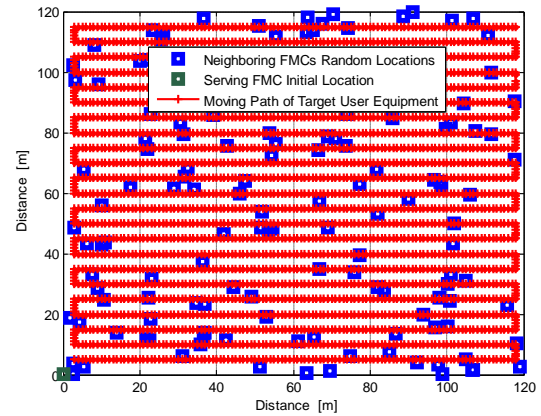
BS - FMC<sub>UE</sub> interference is the transmission of signals from different layers in the network which called cross-layer interference. BS-FMC<sub>UE</sub> interference occurs at downlink when an unwanted signal is received at a FMC<sub>UE</sub> which has been sent from the BS [19-21].

## IV. DOWNLINK SIMULATION SCENARIO FOR VARYING COVERAGE AREA

### A. Scenario Network Layout



(a)



(b)

Figure 1. Floor Plan of (a) Scenario and Network Layout, and (b) Serving FMC Initial Location, Neighbouring FMCs Locations and Moving Path of Target User Equipment

The FMC network has been modeled as an indoor base station that deploys signals in regular sites characterized by the site distance  $d$ . In this scenario we assumed a one level hospital building which is 120 m in the X-axis length and 120 m in the Y-axis width. The inside of the building consists of 1 reception desk (and patient files), 3 emergency diagnostic rooms, 9 doctors rooms, 1 nurses Counter, 2 X-ray rooms, 2 Test lab, one operation room, one extensive care room and 37 patients rooms, hospital facilities and 144 FMCs installed indoors each is serving up to 4 UEs, as shown in the floor plan of Fig. 1(a).

This is a downlink scenario where the main signal is transmitted from the serving FMC to the target UE, while the interference is transmitted from the interferer neighboring FMCs to the target UE. The serving FMC is chosen by calculation as the nearest FMC to the target UE, while the target UE is initiated by X to be 0.2 m and Y to be 0.2 m. This simulation calculates the average interference that comes from every interferer neighboring FMC on the target UE locations at the X and Y grids. The simulation continues by increasing X by 1 m up to 120 m while Y fixed in 1 m and vice-versa. This continues until Y reaches 120 m and X is 120 m. This is repeated within every interferer neighboring FMC increment and added to the previous interference which calculated from the previous interferer neighboring FMCs, as shown in the floor plan of Fig. 1(b). The simulation evaluates the interference, SINR and the probability of connection computed for 1 to 144 interfering FMCs.

### B. Propagation Loss Model

This model is dependent upon the measurements considered at 2 GHz as described by equation (1) [5, 22]. The simulation in this paper concentrates on the results for the indoor residential premises.

$$PL = 50.3 + 31.21 \log_{10}(d) + 3.8 \text{ dB} \quad (1)$$

Equation (1) used to evaluate the path loss power by two measured distances, the first is the distance from the mean signal which is between the serving FMC and the target UE, here  $d$  is the distance between them and it is obtained by the following equation,

$$d = \sqrt{((X(k) - UE(x))^2 + (Y(k) - UE(y))^2)} \quad (2)$$

here  $k$  index of the FMC in  $X(k)$  and  $Y(k)$  is the nearest FMC to the target UE in the  $x$  and  $y$  axis's. While  $UE(x)$  is the coordinate of the target UE in the  $x$  axis, and  $UE(y)$  is the coordinate of the target UE in the  $y$  axis.

The second is the distance from the interference signal which is between the interferers FMCs and the target UE, the distance between every interferer FMC and the target UE is obtained by the following equation.

$$d = \sqrt{((UE(x) - X(k))^2 + (UE(y) - Y(k))^2)} \quad (3)$$

here  $UE(x)$  is the coordinate of the target UE in the  $x$  axis, and  $UE(y)$  is the coordinate of target UE in the  $y$  axis, and  $k$  in  $X(k)$  and  $Y(k)$  is the  $k^{\text{th}}$  interferer FMC in the

$x$  and  $y$  axis's, while  $X(k)$  and  $Y(k)$  is it's coordinate in the  $x$  and  $y$  axis's.

### C. FMC-UE Interference Analysis

Interference occurs in downlink when the signal transmitted from the specific FMC to the target UE overlap in subchannel with the signals which transmits from the neighbouring FMCs. This simulation neglect WiMAX BS to FMC interference, and concentrate on the FMC, neighbouring FMCs and UE interference.

$$S_i = P_i \cdot G_i \cdot L_i \cdot PL_{ix} \cdot G_x \cdot L_x \text{ dB} \quad (4)$$

where  $S_i$  is the received signal by the target UE from the serving FMC,  $P_i$  is the serving FMC transmission power,  $G_i$  is the serving FMC antenna gain,  $L_i$  is the serving FMC cable loss,  $PL_{ix}$  is the path loss between the serving FMC and the target UE,  $G_x$  is the target UE antenna gain,  $L_x$  is the target UE loss.

$$S_j = P_j \cdot G_j \cdot L_j \cdot PL_{jx} \cdot G_x \cdot L_x \text{ dB} \quad (5)$$

here  $S_j$  is the received signals from the interferer FMC by the target UE,  $G_j$  is the interferer neighbouring FMC antenna gain,  $L_j$  is the interferer neighbouring FMC cable loss,  $PL_{jx}$  is the path loss between the interferer neighbouring FMC and the target UE. Our simulation will accumulate to compute the interference value that caused by all interferers neighbouring FMCs on the target UE. The transmitted signal from the specific FMC to the target UE is considered as the mean signal, and the sum of the transmitted signals of all interferers neighbouring FMCs to the target UE as the interference.

$$n = -174 - 30 + 10 \log_{10}(f/SC) \text{ dB} \quad (6)$$

$$\sigma = n + n_F \text{ dB} \quad (7)$$

here,  $n$  is the thermal noise in dB,  $f$  is the Channel bandwidth frequency which is 512 MHz, and  $SC$  is the total subcarrier used which is 512, and  $n_F$  is the noise Figure of the target UE which is 8 dB.  $\sigma$  [4] is the sum of the thermal noise and the target UE noise Figure.

$$\text{SINR} = S_i / (\sum S_j + \sigma) \text{ dB} \quad (8)$$

Where,  $S_i$  is the transmitted signal from the serving FMC to the target UE,  $S_j$  is the accumulation of all the transmitted signals from the interferer FMCs to the target UE [23]. Our simulation would compute the SINR value that is caused by all interferers neighbouring FMCs on the target UE.

## V. SIMULATION RESULTS

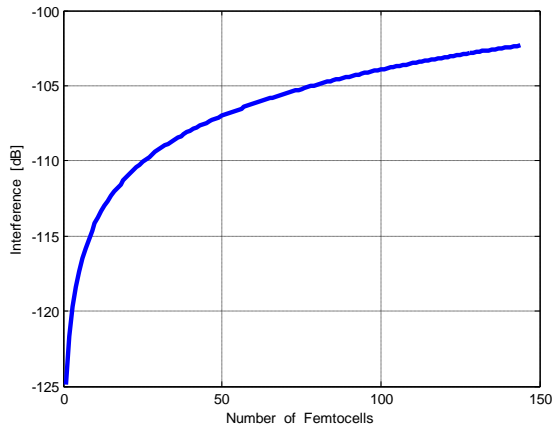
In this study a number of simulations were carried out, each have a number of iterations to calculate the interference at the indoor. The desired FMC coverage distance is suggested to be 10 m in each direction and 10 m by 10 m area will be covered by the individual FMC, here for the whole area we used 144 FMCs. The simulation calculated the downlink interference from the interferers neighboring FMCs to the target UE, where the serving FMC is chosen as the nearest FMC to the target UE.

TABLE II. SUMMARY OF SYSTEM SIMULATION PARAMETERS

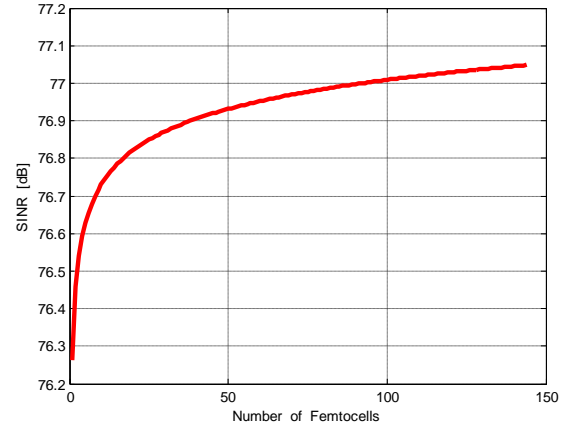
Parameter	Value
Number of FMCs	144
Carrier frequency	3.5 GHz
Channel bandwidth	5 MHz
Total subcarriers	512
Data subcarriers	318
Subchannels	8
Distance of Area	120 m x 120 m
FMC TX power	10 dBm
FMC antenna gain	0 dBi
FMC cable loss	0 dBi
FMC noise Figure	4 dB
UE Tx power	23 dBm
UE antenna gain	0 dBi
UE cable loss	0 dB
UE noise Figure	8 dB

The interference of the target UE is evaluated in the grids of the X and Y axis's by substituting the target UE location and calculates the average interference. The simulation evaluates the interference, SINR, and the probability of connection. The carrier frequency  $f$  was set to 2 GHz, and all other simulation parameters were used as in Table II.

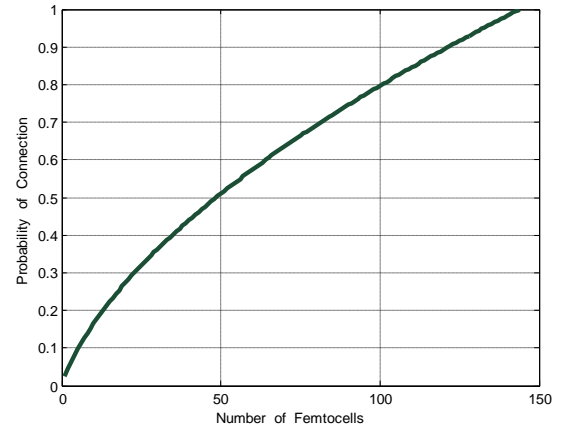
#### A. Interference



(a)



(b)



(c)

Figure 2. FMCs-UE, (a) Interference, (b) SINR and (c) Probability of Connection

The downlink interference is calculated from the interferer neighbouring FMCs to the target UE, at a varied number of FMCs from 1 FMC up to 144 FMCs which is the maximum number of interferers FMCs in this simulation. In Fig. 2(a) the interference increases within the increase of FMCs number. The simulation shows that the interference magnitude increases gradually to be -124.89 dB with 1 FMC, -107 dB in 50 FMCs and -102.32 dB at 144 FMCs which is the maximum number of FMCs.

#### B. SINR

Fig. 2(b) indicates the signal-to-interference and noise ratio SINR, which calculated by the main signal that transmitted from the served FMC to the target UE, and the interference that are accumulated from all the neighboring FMCs to the target UE. The simulation calculates the SINR, at a varied number of FMCs from 1 FMC up to 144 FMCs which is the allowed number of FMCs in our simulation. The SINR increases slightly with the increase of FMCs number. The simulation shows that the minimum SINR reading value is 76.26 dB with 1 FMC

and the maximum SINR reading value is 77.05 dB when the number of FMCs is equal to 144.

C. Probability of Connection

Fig. 2(c) shows the probability of connection at the indoors within 0 dB SINR threshold value and a varied number of FMCs 1 FMC up to 144 FMCs. The probability of connection from the FMCs to the UEs increases approximately in straight deviation trend within the increase in FMCs, for instance in our simulation as shown in Fig. 2(c) the probability of connection is 0.03 (3 %) in one FMC, 0.52 (52 %) in 50 FMCs and finally it is 1.0 (100 %) the best and complete connection when the number of FMCs is 144.

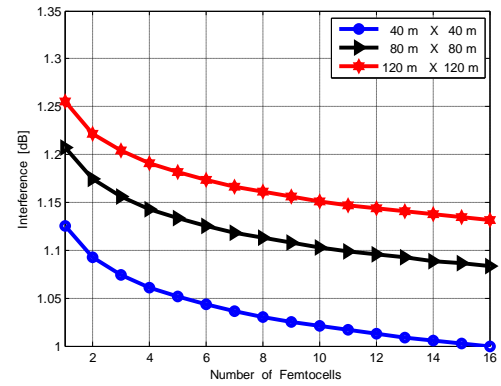
D. Comparison of FMC at Various Indoors Areas

Figs. 3(a)-3(d) show the interference, SINR and the probability of connection for 3 cases, each case consists of different area dimensions and 16 FMCs, the first case curve shows the area dimension of 120 m x 120 m, the second case curve is the area dimension of 80 m x 80 m and the third case curve is the area dimension of 40 m x 40 m.

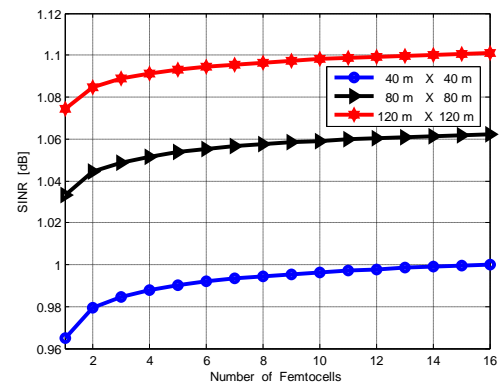
In Fig. 3(a) the interference is raised within the increase of the area dimension and in every case the interference is trend to low down slightly within the increase of FMCs. For instance in our simulation the largest area dimension; which is 120 m x 120 m has the highest interference amongst the 3 areas. Moreover, the interference in the largest area is decreased within the increase of FMCs, the interference with 1 FMC is 1.26 dB, with 10 FMCs the interference is 1.15 dB and with 16 FMCs the interference is 1.13 dB.

In Fig. 3(b) the SINR is raised dramatically within the increase of the area dimension and in every case the SINR is increases slightly within the increase of FMCs number. For instance in our simulation the smallest area dimension; which is 40 m x 40 m has the lowest SINR amongst the three areas. Moreover, the SINR in the smallest area is increased within the increase of FMCs, the SINR with 1 FMC is 0.965 dB, with 5 FMCs the SINR is 0.99 dB and with 16 FMCs the SINR is approximately 1.0 dB.

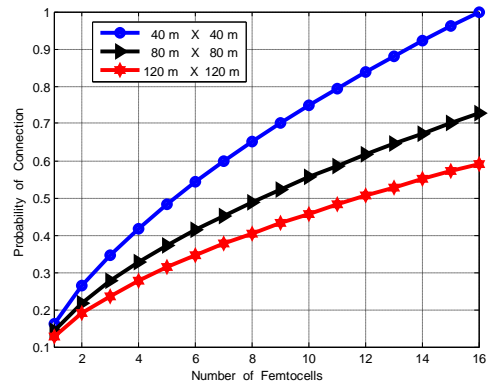
However, in Fig. 3(c) the probability of connection is decreased within the increases in area dimensions and in every case the probability of connection increases within the increase in FMCs number. For instance in the smallest area which is 40 m x 40 m dimensions the probability of connection is the highest amongst the 3 areas. Also, for this area the probability of connection increases within the increase in FMCs number. Therefore, the probability of connection is 0.16 (16 %) in 1 FMC, 0.75 (75 %) in 10 FMCs and finally it is the best connection 1.0 (100 %) when the number of FMCs for this area is 16.



(a)



(b)



(c)

Figure 3. FMCs-UE at Various Area Dimensions, (a) Interference, (b) SINR and (c) Probability of Connection.

E. Comparison of Various SINR in 3-D FMC at 120 m x 120 m

In this study a number of simulations were carried out, each have a number of iterations to calculate the interference and the SINR for various SINR threshold values in dB in the indoors. The best FMC coverage distance is 10 m Omni direction therefore 10 m by 10 m area will be covered by a single FMC. These simulations were run in 3 dimensions in the indoors for the area 120 m x 120 m at 4 scenarios. Scenario1, which contains 18

FMCs, scenario 2 contains 36 FMCs; scenario 3 contains 72 FMCs and scenario 4 which contains 144 FMCs. In all the scenarios the simulation calculated the downlink interference from the interferers neighboring FMCs to the target UE, where the serving FMC is chosen as the nearest FMC to the intersection centre of X and Y axes, while the target UE is initiated by X to be 1 m and Y to be 1 m and continued by increasing X up to 120 m while Y fixed in 1 m then increment Y by 1 m and varied X from 1 m to 120 and so on up to Y reached 120 m and X is 120 m, this is repeated within every FMC increment. Moreover, these simulations are evaluating the probability of connection in 3 dimensions at various SINR threshold values which are 0, 10, 15 and 20 dB.

Table III and Fig. 4 show the probability of connection in 3 dimensions for 18 FMCs at 120 m x 120 m in 0 dB, 10 dB, 15 dB and 20 dB SINR threshold values. The probability of connection in 0 dB started at 70 % and end at 90 % as maximum probability, while it started at 60 % and end at 80 % as maximum probability in 10 dB. Moreover, the probability of connection in 15 dB started at 20 % and end at 60 % as maximum probability, while it started at 10 % and end at 50 % as maximum probability in 20 dB.

Table IV and Fig. 5 show the probability of connection in 3 dimensions for 36 FMCs at 120 m x 120 m in 0 dB, 10 dB, 15 dB and 20 dB SINR threshold values. The probability of connection in 0 dB and 10 dB is good and it is 100 %, while it started at 80 % and ended at 90 % as maximum probability in 15 dB. Moreover, the probability of connection in 20 dB started at 50 % and ended at 85 % as maximum probability.

Table V and Fig. 6 show the probability of connection in 3 dimensions for 72 FMCs at 120 m x 120 m in 0 dB, 10 dB, 15 dB and 20 dB SINR threshold values. The probability of connection in 0 dB and 10 dB is good and it is 100 %, while it is 90 % probability in 15 dB. Moreover, the probability of connection in 20 dB started at 80 % and end at 90 % as maximum probability.

Table VI and Fig. 7 show the probability of connection in 3 dimensions for 144 FMCs at 120 m x 120 m in 0 dB, 10 dB, 15 dB and 20 dB SINR threshold values. The simulation presented that the probability of connection in these threshold values 100 %.

Table VII presents the summary for the probability of connection in 3 dimensions for 18, 36, 72 and 144 FMCs distributions at 120 m x 120 m, within various SINR threshold values which are 0 dB, 10 dB, 15 dB and 20 dB. The simulation illustrated that the probability of connection for the number of 18 FMCs distributions is good in 0 dB and 5 dB SINR threshold values, while the probability of connection is weak in 15 dB and 20 dB. In addition, the simulation illustrated that the probability of connection for the number of 36 FMCs distributions is high in 0 dB and 5 dB SINR threshold values, while the probability of connection is good in 15 dB SINR threshold value and between weak and good in 20 dB SINR threshold value. Moreover, the simulation illustrated that the probability of connection for the number of 72 FMCs

distributions is high in 0 dB and 10 dB SINR threshold values, while the probability of connection is good in 15 dB and 20 dB SINR threshold values. Finally, the simulation illustrated that the probability of connection for the number of 144 FMCs distributions is high in all the SINR threshold values which are 0 dB, 10 dB, 15 dB and 20 dB.

TABLE III. PROBABILITY OF CONNECTION FOR 18 FMCs IN 3-DIMENSIONS

Threshold SINR Value	% for The Probability of Connection
0 dB	70 % – 90 %
10 dB	60 % – 80 %
15 dB	20 % – 60 %
20 dB	10 % – 50 %

TABLE IV. PROBABILITY OF CONNECTION FOR 36 FMCs IN 3-DIMENSIONS

Threshold SINR Value	% for The Probability of Connection
0 dB	100 %
10 dB	100 %
15 dB	80 % – 90 %
20 dB	50 % – 85 %

TABLE V. PROBABILITY OF CONNECTION FOR 72 FMCs IN 3-DIMENSIONS

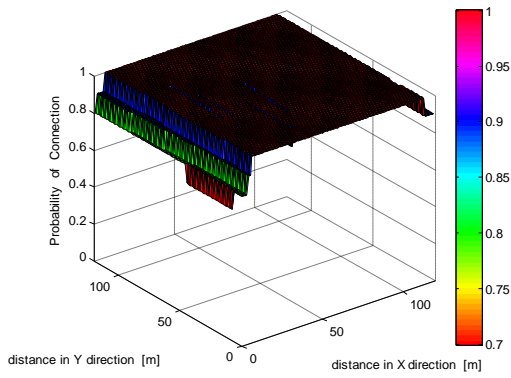
Threshold SINR Value	% for The Probability of Connection
0 dB	100 %
10 dB	100 %
15 dB	90 %
20 dB	80 % – 90 %

TABLE VI. PROBABILITY OF CONNECTION FOR 144 FMCs IN 3-DIMENSIONS

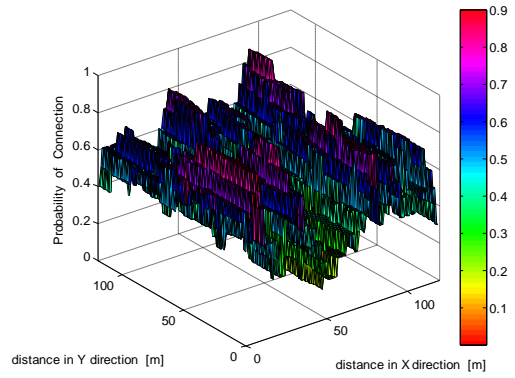
Threshold SINR Value	% for The Probability of Connection
0 dB	100 %
10 dB	100 %
15 dB	100 %
20 dB	100 %

TABLE VII. SUMMARY FOR THE PROBABILITY OF CONNECTION IN 3-DIMENSIONS FOR THE AREA 120 X 120 M

Threshold SINR in	Number of FMCs			
	36 FMCs	36 FMCs	72 FMCs	144 FMCs
0 dB	70 % – 90 %	100 %	100 %	100 %
10 dB	60 % – 80 %	100 %	100 %	100 %
15 dB	20 % – 60 %	80 % – 90 %	90 %	100 %
20 dB	10 % – 50 %	50 % – 85 %	80 % – 90 %	100 %

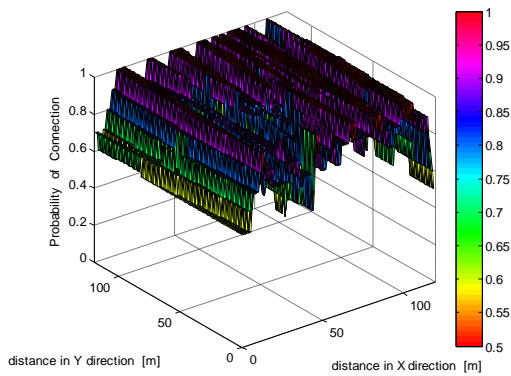


(a)

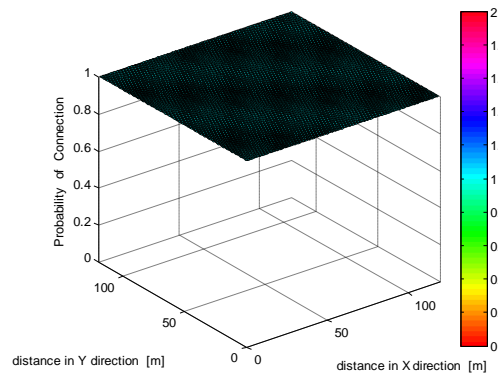


(d)

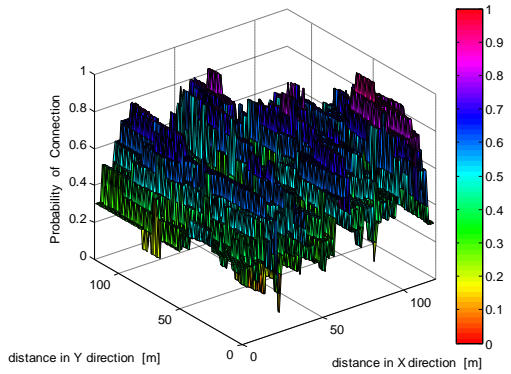
Figure 4. The Probability of Connection in 18 FMCs, (a) 0 dB SINR threshold value, (b) 10 dB SINR threshold value, (c) 15 dB SINR threshold value and (d) 20 dB SINR threshold value



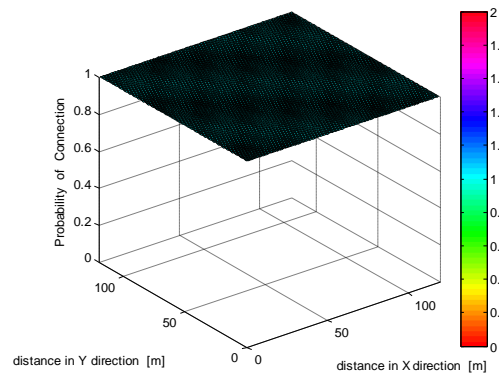
(b)



(a)



(c)



(b)

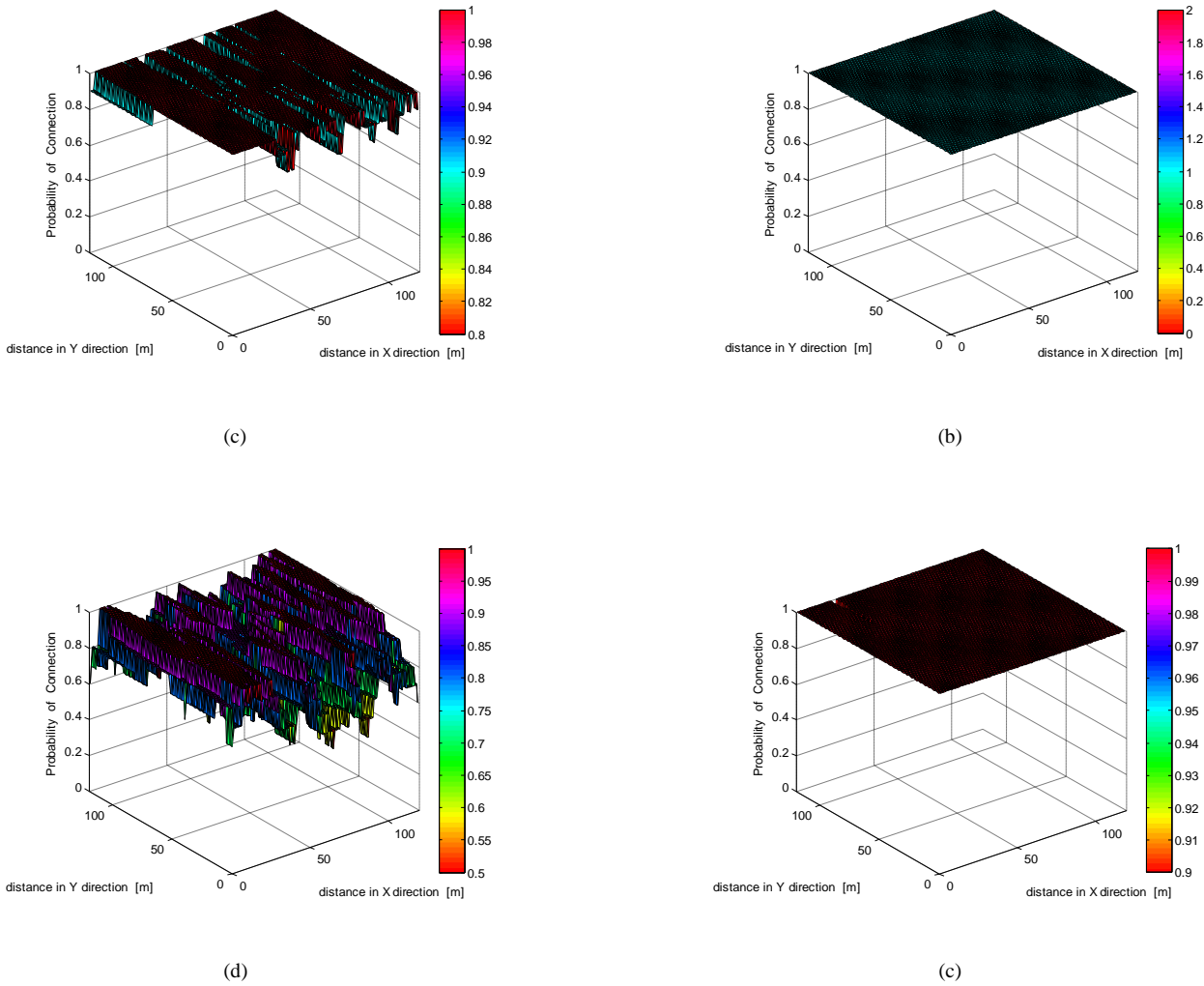


Figure 5. The Probability of Connection in 36 FMCs, (a) 0 dB SINR threshold value, (b) 10 dB SINR threshold value, (c) 15 dB SINR threshold value and (d) 20 dB SINR threshold value

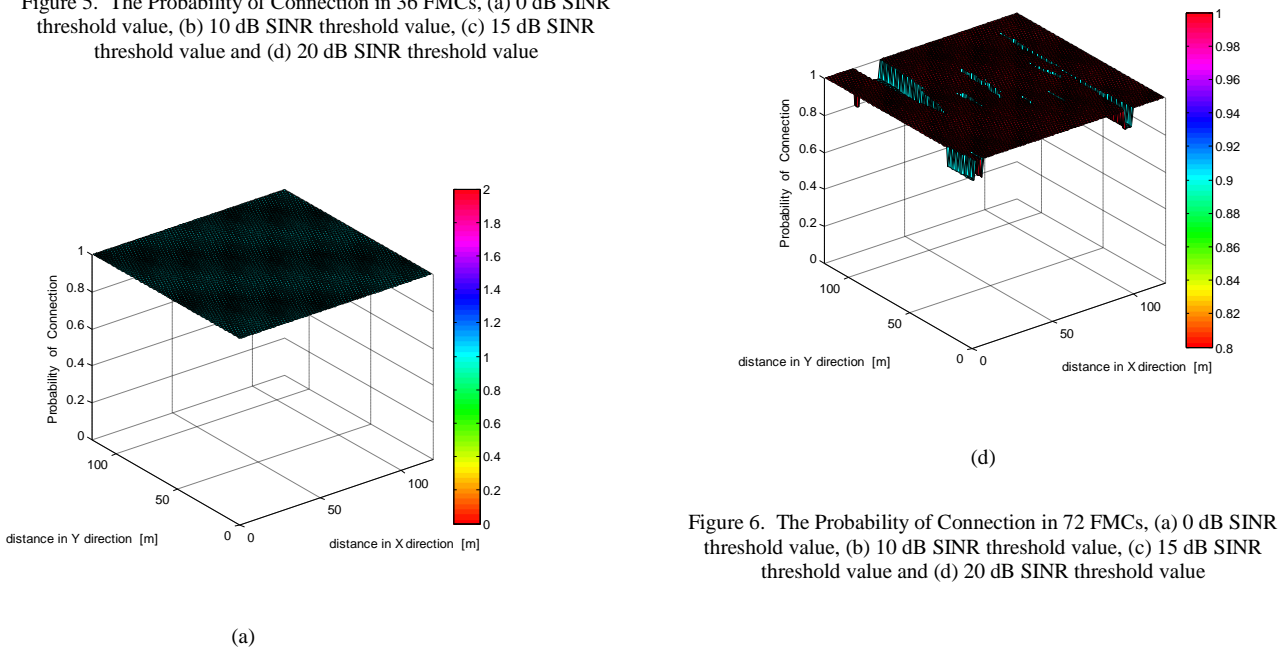
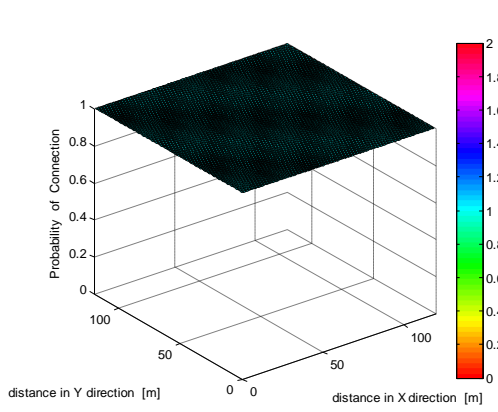
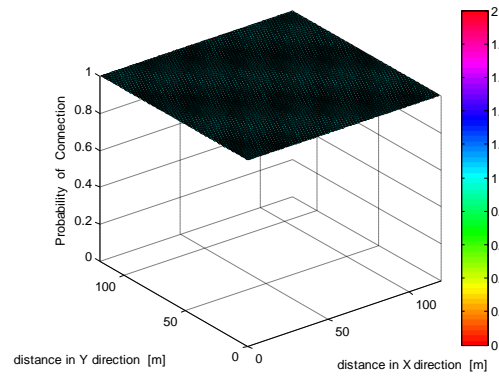


Figure 6. The Probability of Connection in 72 FMCs, (a) 0 dB SINR threshold value, (b) 10 dB SINR threshold value, (c) 15 dB SINR threshold value and (d) 20 dB SINR threshold value



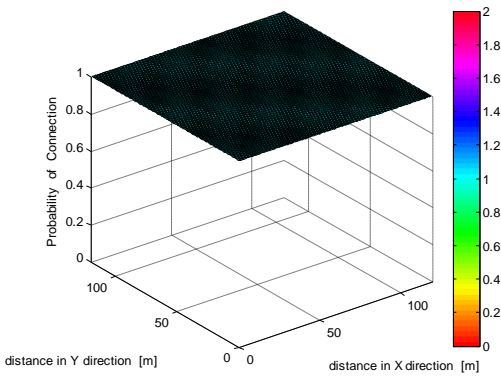


(a)

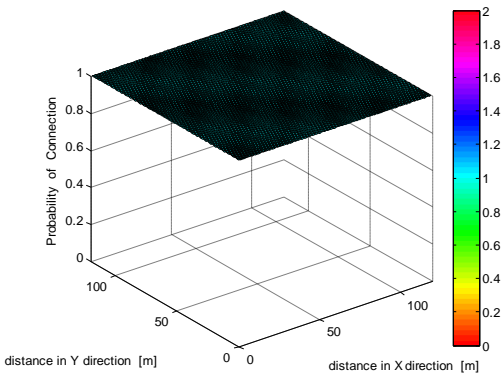


(d)

Figure 7. The Probability of Connection in 144 FMCs, (a) 0 dB SINR threshold value, (b) 10 dB SINR threshold value, (c) 15 dB SINR threshold value and (d) 20 dB SINR threshold value



(b)



(c)

## VI. CONCLUSIONS

The downlink interference occurred when the serving FMC and the neighbor FMC are transmitted at the same subchannel. In this paper we have investigated the downlink of FMCs deployment strategies indoors for mobile radio networks in 2 scenarios.

This simulation calculates the interference, SINR and the probability of connection for varied number of FMCs 1 up to 144 FMCs in fixed area dimensions which is 120 m x 120 m. Therefore, the probability of connection from the FMCs to the UEs increases approximately in straight line trend within the increase in FMCs. We have presented the interference, SINR and the probability of connection for 3 cases, each case consists of different area dimensions and 16 FMCs, the first case curve shows the area dimension of 120 m x 120 m, the second case curve is the area dimension of 80 m x 80 m and the third case curve is the area dimension of 40 m x 40 m. The interference is raised within the increase of the area dimension and in every case the interference is trend to low down slightly within the increase of FMCs, while the SINR is raised within the increase of the area dimensions or within the increase of FMCs. The probability of connection is decreases within the increased in area dimension and increases within the increase in FMCs number.

Moreover, the work in this paper presented the probability of connection in 3 dimensions for 18, 36, 72 and 144 FMCs distributions at 120 m x 120 m, within various SINR threshold values which are 0 dB, 10 dB, 15 dB and 20 dB. The simulation illustrated that the probability of connection is high and perfect for the number of 144 FMCs distributions, while the probability of connection is the worst for the number of 18 FMCs distributions especially when SINR threshold values is

more than 10 dB. Moreover, the probability of connection is high and perfect for the numbers of 36 FMCs and 72 FMCs distributions when SINR threshold values is less than 10 dB and not perfect or sometimes weak when SINR threshold values is more than 10 dB.

The interference can be managed if appropriate number of FMCs and different subchannels are used. Furthermore, we have presented that by using FMCs indoors the capacity and coverage increased on downlink because the UEs served by FMCs can process more data rates than by BS.

## REFERENCES

- [1] R. Madan, A. Sampath, A. Khandekar, J. Borran, and N. Bhushan, "Distributed interference management and scheduling in LTE-A femto networks," in *Global Telecommunications Conference (GLOBECOM 2010)*, 2010 IEEE, 2010, pp. 1-5.
- [2] S. F. Hasan, N. H. Siddique, and S. Chakraborty, "Femtocell versus WiFi-A survey and comparison of architecture and performance," in *Wireless Communication, Vehicular Technology, Information Theory and Aerospace & Electronic Systems Technology*, 2009. *Wireless VITAE 2009. 1st International Conference on*, 2009, pp. 916-920.
- [3] A. Golaup, M. Mustapha, and L. B. Patanapongpibul, "Femtocell access control strategy in UMTS and LTE," *Communications Magazine, IEEE*, vol. 47, pp. 117-123, 2009.
- [4] J. Zhang and G. De la Roche, *Femtocells: technologies and deployment*: Wiley Online Library, 2010.
- [5] J. Boccuzzi and M. Ruggiero, *Femtocells: design & application*: McGraw-Hill Professional, 2010.
- [6] S. Prasad and R. Baruah, "Femtocell mass deployment: Indian perspective," in *Anti-counterfeiting, Security, and Identification in Communication*, 2009. *ASID 2009. 3rd International Conference on*, 2009, pp. 34-37.
- [7] I. O. Kennedy, P. Scanlon, and M. M. Buddhikot, "Passive steady state rf fingerprinting: A cognitive technique for scalable deployment of co-channel femto cell underlays," in *New Frontiers in Dynamic Spectrum Access Networks*, 2008. *DySPAN 2008. 3rd IEEE Symposium on*, 2008, pp. 1-12.
- [8] S. Saunders, S. Carlaw, A. Giustina, R. R. Bhat, V. S. Rao, and R. Siegberg, *Femtocells: opportunities and challenges for business and technology*: Wiley, 2009.
- [9] M. Simsek, T. Akbudak, B. Zhao, and A. Czylik, "An LTE-femtocell dynamic system level simulator," in *Smart Antennas (WSA)*, 2010 *International ITG Workshop on*, 2010, pp. 66-71.
- [10] Z. R. Bharucha, "Ad hoc wireless networks with femto-cell deployment: a study," 2010.
- [11] T. Alade and H. Zhu, "Joint Signal Processing in Femtocell Based Distributed Antenna Systems in High Buildings," in *Vehicular Technology Conference Fall (VTC 2010-Fall)*, 2010 IEEE 72nd, 2010, pp. 1-5.
- [12] V. Chandrasekhar, J. Andrews, and A. Gatherer, "Femtocell networks: a survey," *Communications Magazine, IEEE*, vol. 46, pp. 59-67, 2008.
- [13] M. I. Rahman, E. Dahlman, D. Astely, A. Wallén, and L. R. Wilhelmsson, "A Study of UE-to-UE Interference between TDD Systems," in *Vehicular Technology Conference (VTC Spring)*, 2012 IEEE 75th, 2012, pp. 1-5.
- [14] D. Choi, P. Monajemi, S. Kang, and J. Villaseñor, "Dealing with loud neighbors: The benefits and tradeoffs of adaptive femtocell access," in *Global Telecommunications Conference*, 2008. *IEEE GLOBECOM 2008. IEEE*, 2008, pp. 1-5.
- [15] C. M. de Lima, M. Bennis, K. Ghahboosi, and M. Latvaaho, "Interference management for self-organized femtocells towards green networks," in *Personal, Indoor and Mobile Radio Communications Workshops (PIMRC Workshops)*, 2010 IEEE 21st International Symposium on, 2010, pp. 352-356.
- [16] F. Richter, A. J. Fehske, and G. P. Fettweis, "Energy efficiency aspects of base station deployment strategies for cellular networks," in *Vehicular Technology Conference Fall (VTC 2009-Fall)*, 2009 IEEE 70th, 2009, pp. 1-5.
- [17] V. Chandrasekhar, M. Kountouris, and J. G. Andrews, "Coverage in multi-antenna two-tier networks," *Wireless Communications, IEEE Transactions on*, vol. 8, pp. 5314-5327, 2009.
- [18] D. López-Pérez, G. de la Roche, A. Valcarce, A. Juttner, and J. Zhang, "Interference avoidance and dynamic frequency planning for WiMAX femtocells networks," in *Communication Systems*, 2008. *ICCS 2008. 11th IEEE Singapore International Conference on*, 2008, pp. 1579-1584.
- [19] M. Yavuz, F. Meshkati, S. Nanda, A. Pokhariyal, N. Johnson, B. Raghathan, et al., "Interference management and performance analysis of UMTS/HSPA+ femtocells," *Communications Magazine, IEEE*, vol. 47, pp. 102-109, 2009.
- [20] H. Claussen, "Performance of macro-and co-channel femtocells in a hierarchical cell structure," in *Personal, Indoor and Mobile Radio Communications*, 2007. *PIMRC 2007. IEEE 18th International Symposium on*, 2007, pp. 1-5.
- [21] M. Z. Chowdhury, W. Ryu, E. Rhee, and Y. M. Jang, "Handover between macrocell and femtocell for UMTS based networks," in *Advanced Communication Technology*, 2009. *ICACT 2009. 11th International Conference on*, 2009, pp. 237-241.
- [22] S. Y. Seidel and T. S. Rappaport, "914 MHz path loss prediction models for indoor wireless communications in multifloored buildings," *Antennas and Propagation, IEEE Transactions on*, vol. 40, pp. 207-217, 1992.
- [23] T. Zahir, K. Arshad, A. Nakata, and K. Moessner, "Interference management in femtocells," 2012.



**Author 1 Mohammed Alshami** is currently a PhD student in System Level Integration and Wireless communications. His interests include the research of Novel Techniques to Enhance WiMAX Throughput for Cell-edge Users using a combination of MIMO, femtocell and SDD scheme. His project will

study radio propagation issues in wireless communications networks. It will address how radio propagation in different environments affects the performance and data capacity of mobile communications systems. It will also consider different cell types, such as large, high power macro-cells and smaller, low power femto-cells. The project will also study interference issues in femto-cell networks, addressing how interference can degrade performance. Multiple antenna technologies will also be studied as a means to reduce interference observed at wireless receivers and to thus optimize performance. He obtained his bachelor and master degrees in Computer Engineering from King Abdulaziz University, Jeddah, Kingdom of Saudi Arabia.



**Author 3 Professor John S. Thompson** was appointed as a lecturer at what is now the School of Engineering at the University of Edinburgh in 1999. He was recently promoted to a personal chair in Signal Processing and Communications. His research interests currently include energy efficient

communications systems, antenna array techniques and multihop wireless communications. He has published over 200 papers to date including a number of invited papers, book chapters and tutorial talks, as well as co-authoring an undergraduate textbook on digital signal processing. From 2012-2014 he will serve as member-at-large for the Board of Governors of the IEEE Communications Society. He was technical programme co-chair for the IEEE Globecom Conference in Miami in 2010 and recently served in the same role for the IEEE Vehicular Technology Conference Spring in Dresden in 2013.



**Author 2 Professor Tughrul Arslan** holds the Chair of Integrated Electronic Systems in the School of Engineering, University of Edinburgh, U.K. He is a member of the Integrated Micro and Nano Systems (IMNS) Institute and leads the Embedded and Wireless Systems Group in the University. His current research

focuses on enhancing personal mobility and the design of high performance embedded wireless systems. He has supervised over 30 successful PhD research thesis and is the author of over 450 refereed research papers and the inventor of over 15 patents in these areas. Prof. Arslan was an Associate Editor for the IEEE Transactions on Circuits and Systems I (2005-2006), IEEE Transactions on Circuits and Systems II (2008-2009), a member of the IEEE CAS executive Committee on VLSI Systems and Applications (1999 to date), and is a member of the steering and technical committees of a number of international conferences (see the conferences link). He is a co-founder of the NASA/ESA conference on Adaptive Hardware and Systems (AHS) and currently serves as a member of its steering committee.